Relaxation pathway confinement in glassy dynamics

J. A. Rodriguez Fris, M. A. Frechero, and G. A. Appignanesi

Citation: The Journal of Chemical Physics **141**, 114905 (2014); doi: 10.1063/1.4895608
View online: http://dx.doi.org/10.1063/1.4895608
View Table of Contents: http://scitation.aip.org/content/aip/journal/jcp/141/11?ver=pdfcov
Published by the AIP Publishing

Relaxation pathway confinement in glassy dynamics

J. A. Rodriguez Fris,[a] M. A. Frechero, and G. A. Appignanesi
Sección Fisicoquímica, INQUISUR-UNS-CONICET, Universidad Nacional del Sur, Av. Alem 1253, 8000 Bahía Blanca, Argentina

(Received 29 March 2014; accepted 2 September 2014; published online 16 September 2014)

We compute for an archetypical glass-forming system the excess of particle mobility distributions over the corresponding distribution of dynamic propensity, a quantity that measures the tendency of the particles to be mobile and reflects the local structural constraints. This enables us to demonstrate that, on supercooling, the dynamical trajectory in search for a relaxation event must deal with an increasing confinement of relaxation pathways. This "entropic funnel" of relaxation pathways built upon a restricted set of mobile particles is also made evident from the decay and further collapse of the associated Shannon entropy. © *2014 AIP Publishing LLC*. [http://dx.doi.org/10.1063/1.4895608]

INTRODUCTION

The nature of the glass transition, that is, the dramatic dynamic slowing down that a glass-forming system experiences when supercooled below its melting point, continues to be one of the major open questions in condensed-matter physics.[1–31] A main ingredient for glassy dynamics is the presence of dynamical heterogeneities.[1,3,32,33] According to this description, the relaxation slows down by a particle-caging effect whose lifetime enormously increases as temperature is lowered within the supercooled regime towards the critical temperature of mode-coupling theory, T_c,[34–43] while the distribution of particle mobility becomes inhomogeneous or non-gaussian.[32] Additionally, the structural relaxation (or α relaxation) has been shown to be accomplished by means of sporadic bursts in mobility comprising the collective motion of a significant number of particles involved in a relatively compact cluster, or d-cluster.[28,33,44,45] In turn, the configuration-space counterpart of this real-space description is provided by the landscape paradigm:[2,33] At low temperatures such that equilibration within local minima is fast compared to transitions between them, the dynamics of the system can be described as an exploration of its Potential Energy Landscape, PEL. Any given configuration of the PEL can be minimized to reach its local basin of attraction or inherent structure (IS). Thus, the PEL can be decomposed in an extremely large collection of ISs which, in turn, are arranged in superstructures called Metabasins, MBs. A MB is a group of closely related or similar ISs which is separated from other MBs by a long range particle rearrangement.[2,33,46] Contrasting with the situation at higher temperatures when the system performs a non-glassy free-diffusion given that the system has enough kinetic energy to easily overcome the barriers of the PEL, the regime that sets in upon supercooling has been termed "landscape influenced"[2] since the trajectory is subject to confinement within the local MB, with MB transitions triggered by a d-cluster event.[33,44,45,49] Approaching T_c, the dynamical trajectory gets increasingly MB-confined (MB-residence times grow significantly) and thus, the exploration of the PEL becomes "landscape dominated."[2] Additionally, a third main brush-stroke for the description of glassy dynamics came with the introduction of the concept of dynamic propensity. This quantity represents the tendency of the particles to be mobile, reflecting the constraints imposed by the local structure on the dynamics.[10,47] Specifically, dynamic propensity is defined over the isoconfigurational ensemble, IC, consisting of many separate simulation runs over a fixed time interval, all originating from the same particle configuration but with momenta chosen randomly from the corresponding Maxwell-Boltzmann distribution at the appropriate temperature. The propensity for motion of each particle is obtained by averaging its squared displacements over all the separate runs (that is, averaging over the IC; see equation below). Thus, such value represents the ensemble characterization of the particle's capacity for movement from a specific initial configuration. The distribution of particle propensities has been shown to be sharp at high temperature but to get progressively broader with supercooling,[10,47,48] when it becomes spatially heterogeneous and displays high-propensity particles arranged in relatively compact clusters (which have also been related to the local soft modes of the sample).[10,47,50] It has also been shown that the propensity pattern decorrelates by means of d-cluster events (i.e., by MB transitions) and, thus, the influence of the structure on dynamics extends only at the local MB level while the long-time (diffusive) dynamics of the system can be described as a random walk on MBs.[46,49,50] Within the aforementioned framework, our present work focuses on the relationship between propensity and average dynamics. Thus, by monitoring the dependence with temperature of such relationship we reveal the confinement of trajectories in phase space that takes place upon supercooling.

METHODOLOGY

We performed a series of molecular dynamics (MD) simulations for a paradigm model of fragile glass former: a system consisting of a mixture of 80% A and 20% B particles within a three-dimensional box, the size of the A particles

[a]Electronic mail: rodriguezfris@uns.edu.ar

(σ_{AA}) being 10% larger than the B ones. The interaction between two atoms of type α and β is given by[34]

$$V_{\alpha\beta}(r) = 4\epsilon_{\alpha\beta}\left[\left(\frac{\sigma_{\alpha\beta}}{r}\right)^{12} - \left(\frac{\sigma_{\alpha\beta}}{r}\right)^{6}\right], \quad (1)$$

where $\alpha, \beta \in \{A, B\}$ and r is the distance between α and β. The LJ parameters used were $\epsilon_{AA} = 1.0$, $\sigma_{AA} = 1.0$, $\epsilon_{AB} = 1.5$, $\sigma_{AB} = 0.8$, $\epsilon_{BB} = 0.5$, and $\sigma_{BB} = 0.88$. These interactions have been truncated and shifted at $r_{\text{cutoff}} = 2.5\sigma_{\alpha\beta}$. In the following, we will use σ_{AA} as units of length, and measure time in units of $(m\sigma_{AA}^2/48\epsilon_{AA})^{1/2}$. The equations of motion were solved for the NVE ensemble at a particle density of 1.2, using the velocity form of the Verlet algorithm with a time step of 0.02 for $T < 1$ and 0.01 for $T \geq 1$. We note that all the quantities we calculate below involve only the A particles; on average these particles are slower than the B particles. We carried out simulation runs after equilibration for a range of temperatures from $T = 3.0$ to $T = 0.446$ (the critical temperature of the Mode Coupling theory for this system has been estimated to be $T_c = 0.435$[34–43]). The systems were always equilibrated for timescales much larger than the corresponding α-relaxation time, τ_α (for the lowest temperatures we equilibrated for timescales almost two orders of magnitude larger than τ_α). We also carefully tested equilibration by monitoring thermodynamic and dynamical quantities in order to discard drifts during the runs. For example, the value of τ_α measured at different times during the runs after equilibration does not present any significant change (for systems that are not properly equilibrated τ_α is expected to increase with time towards its equilibrium value since the system relaxes faster when not equilibrated). We employed $N = 1000$ (but we note that systems of size $N = 8000$ gave similar results).

To calculate propensities we employed the isoconfigurational ensemble (IC) method introduced in Ref. 47 by performing a series of 200 equal length MD runs from the same initial configuration, that is, always the same structure (the same particle positions) but each one with different initial particle momenta chosen at random from the appropriate Maxwell-Boltzmann velocity distribution. We then calculated the dynamic propensity as Ref. 47 $P_i = \langle \Delta\mathbf{r}_i^2(t)\rangle_{\text{IC}}$, (where $\langle\cdots\rangle_{\text{IC}}$ indicates an average over the IC and $\Delta\mathbf{r}_i^2(t) = (\mathbf{r}_i(t) - \mathbf{r}_i(0))^2$ is the squared displacement of particle i in such time interval). Since this quantity is calculated by averaging over different trajectories originated from a fixed initial configuration, it represents the tendency of the particles to move from such initial configuration and thus reflects the constraints imposed by the initial structure on dynamics. We used a short timescale $t = 0.1 \cdot t^*$ and also $t = t^*$ (the spatial distribution of propensity, for times not much larger than τ_α, does not depend on such choice since it reflects a property of the initial configuration[49–51]). t^* represents a characteristic timescale of this system: The timescale of maximum inhomogeneous (non-gaussian) behavior marks the end of the caging regime and the onset of the α-relaxation.[32] t^* depends strongly on temperature (it increases quickly towards T_c[32,33]) and has been shown to provide an estimate of the MB residence time.[32,33] For each T we stored 160 configurations, with consecutive configurations separated by $10 \cdot t^*$. The ICs were performed from these stored configurations and each IC comprised 200 trajectories. We then averaged results from all the 160 ICs (this averaging is necessary since we have already demonstrated that a given IC represents the structural constraints of the local MB where the systems are temporarily confined, and there is a whole distribution of MB sizes and MB residence times[50]).

In turn, we also calculated the distribution of particle squared displacements (without any previous IC averaging): $\Delta\mathbf{r}_i^2(t)$. At any given temperature, this function was calculated by considering explicitly the displacement of each particle within each of the 200 trajectories and for each of the 160 ICs. Given the large statistics provided by using many ICs, the resulting squared-displacement distribution (SDD) is identical to the result when the function is calculated in the usual way, that is, by collecting displacements from many independent single trajectories (no IC method at all), as is done to get van Hove function (normalized distribution of particle displacements). We note that the SDD and the propensity distribution (PD) we calculate share the same data (and hence, have the same mean value). However, the SDD calculation does not imply any averaging (each particle from each trajectory contributes individually to the SDD, which amounts to $800 \times 200 \times 160$ total data: 800 A particles, 200 IC trajectories, and 160 IC ensembles). On the contrary, the PD implies an isoconfigurational averaging (that is, the contribution of each particle is previously averaged over the 200 trajectories of the corresponding IC to get a propensity value and thus, the total number of data of the PD is 800×160).

RESULTS

In Figure 1, we show the comparison of the PD and the SDD for two selected temperatures, $T = 2.0$ and $T = 0.446$, and for $t = 0.1 \cdot t^*$ and $t = t^*$. From such figure it is evident that at high temperatures the SDD and the PD are very different, with the latter being sharp and decaying quickly while the former is broader, presenting a large tail at large displacements. However, we can also learn that at low T the PD is much broader (as already noted[47]) and, more importantly, that the PD tends to follow the decay of the SDD at large $\Delta\mathbf{r}^2$ values. This tendency of the PD to flatten towards the long tail decay of the SDD is more evident for $0.1 \cdot t^*$ than for t^*. This discrepancy should be attributed to the fact that at t^* some trajectories of the IC might have abandoned the local MB of the PEL and the particles might have lost memory of the initial structure. At the beginning, the different trajectories of the IC are confined to the same MB but when they abandon it by means of a d-cluster[33] they reach different neighboring MBs (since the system has many available) and each such MB has now a different propensity map.[50,51] In other words, at t^* the propensity calculation begins to show signs of the loss in heterogeneity that becomes very pronounced at larger times. For this reason, in what follows we only provide results for the neater situation, $0.1 \cdot t^*$. However, the results for t^* are similar. Any given high-propensity particle contributes to the tail of the SDD with the largest displacements between the ones it presents in the different 200 trajectories of the ICs. However, its contribution to the PD implies an averaging over all the

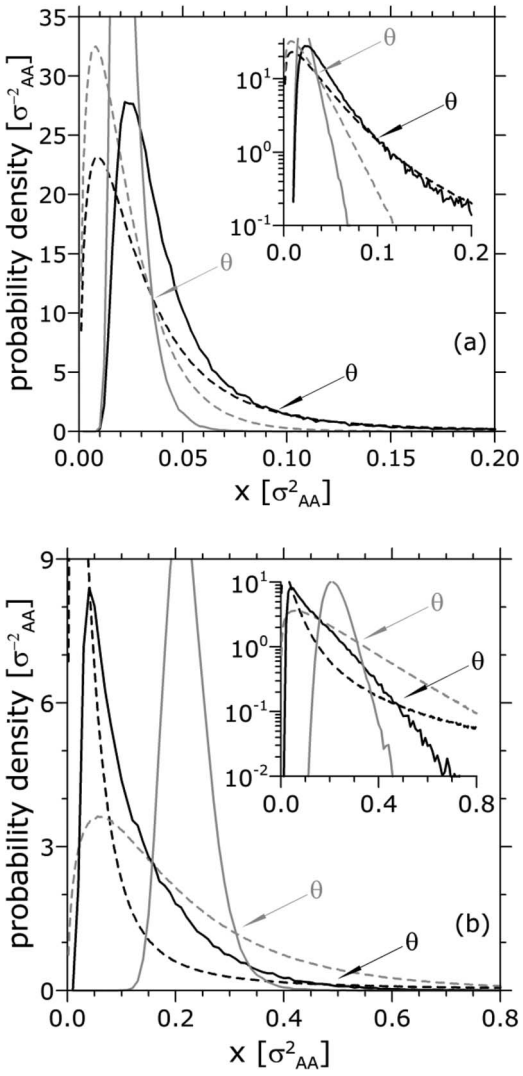

FIG. 1. Comparison of the SDD (squared-displacement distribution, dashed lines) and the PD (propensity distribution, solid lines) for $T = 2.0$ (gray) and $T = 0.446$ (black). (a) $t = 0.1 \cdot t^*$, (b) $t = t^*$. θ is the second intersection between the SDD and the PD. The abscissas X is squared displacement or propensity of a particle A. The tendency of the propensity distribution to follow the long tail decay of the SDD at low temperatures is remarkable. The insets present the same curves in logarithmic representation.

200 trajectories of the IC. Thus, the conspicuous tendency of the PD to resemble the long $\Delta\mathbf{r}^2$ decay of the SDD at low T speaks of the fact that the sets of mobile particles tend to be similar for all the trajectories of the IC. In contrast, the sharp distribution at high T indicates that the sets of mobile particles differ significantly from one IC trajectory to another. We thus decided to calculate the $\Delta\mathbf{r}^2$ value of the second intersection between the SDD and the PD (the intersection at long $\Delta\mathbf{r}^2$ values), which we call θ (see Figure 1 for an estimation of this value for a couple of extreme temperatures). We note that the insets, the logarithmic plots, show a behavior consistent with the one already found by Chaudhuri *et al.*[52] However, here we used squared distributions instead of the linear ones.[52]

The value θ, that signals very mobile particles, allows one to calculate the "excess" ξ of the SDD over the PD, which we define as $\xi = \phi - \omega$, where $\phi = \int_\theta^\infty \mathrm{SDD} \cdot \mathrm{d}\Delta\mathbf{r}^2$ and $\omega = \int_\theta^\infty \mathrm{PD} \cdot \mathrm{d}P$. We display the T dependence of ξ in

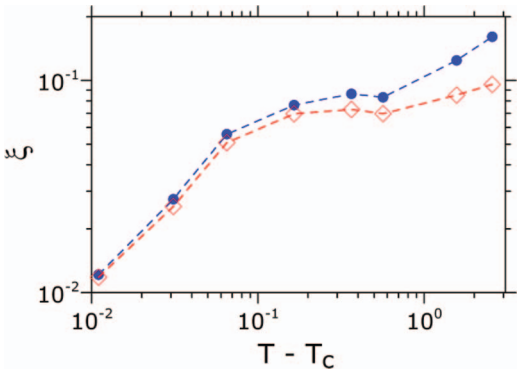

FIG. 2. Temperature dependence of the excess ξ of the squared-displacement distributions (SDD) over the propensity distributions (PD) after θ. Circles: $t = 0.1 \cdot t^*$. The open diamonds represent the same case of $t = 0.1 \cdot t^*$ (circles) but when θ is the value above which the SDD curve, at each T, presents an area equal to 0.1.

Figure 2. The value of ξ measures how different from each other are the sets of mobile particles exhibited by the different trajectories of the IC. Ideally, if the long tail decay of the PD matched perfectly the SDD function, this would mean that the more mobile particles would be the same and would move equally in all the trajectories of the IC. From Figure 2 we can learn that at high temperatures the trajectories of the IC present different sets of mobile particles, a fact that speaks of the existence of plenty of different relaxation pathways. However, below $T \approx 1$ this function begins to decay quickly and somehow tends to collapse at low temperature values approaching T_C. This means that the sets of mobile particles for each IC trajectory tend to be more and more similar to each other as temperature lowers. In other words, as T decreases, the trajectory needs to reach a similar relaxation event. From our previous results linking propensity with d-clusters and MBs,[50] we know that the different trajectories of the IC (diverging trajectories from a common structural origin) explore the local MB in different ways in order to find a d-cluster to perform a transition to another MB, an event that triggers the α relaxation and decorrelates the PD pattern. In the light of the present results it is evident that, as T decreases the trajectory has a fewer number of relaxation pathways available, that is, it can reach fewer events capable of producing the exit from the local MB. It is interesting that the change in behavior at $T \approx 1$ evident from Figure 2 coincides with the change in exploration of the PEL from a free-diffusion to a "landscape influenced" regime, as found previously.[2] In turn, the abrupt decay as T is furthermore decreased is also consistent with the estimated onset of a "landscape dominated" regime around $T_c = 0.435$ within such description.[2] To test the robustness of our finding, we also performed a calculation for a larger system of $N = 8000$ particles and obtained very similar results. We also used a different definition of the value θ as the value beyond which, at each T, the area of the SDD amounts to 0.1 (that is, the 10% of the more mobile particles). For each T and for the IC of length $t = 0.1 \cdot t^*$ we calculated the excess area of the SDD curve over the corresponding PD curve. This result, also displayed in Figure 2 shows the same tendency as the curve with the former definition of θ. Other choices of θ close to this value also give similar results. The same behavior, for t

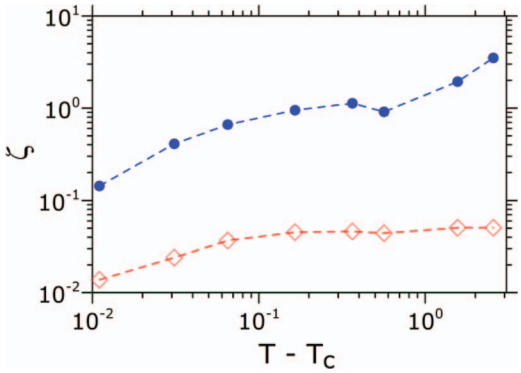

FIG. 3. Temperature dependence of the relative (to PD) excess ζ of the squared-displacement distributions (SDD) over the propensity distributions (PD) after θ. Circles: $t = 0.1 \cdot t^*$. The open diamonds represent the same case of $t = 0.1 \cdot t^*$ (circles) but when θ is the value above which the SDD curve, at each T, presents an area equal to 0.1.

$= 0.1 \cdot t^*$ and for both definitions of θ, can also be seen in Figure 3 but for function $\zeta = (\phi - \omega)/\omega$. ζ is ξ relative to ω, to be free of the absolute sizes of the integrals.

The clear correlation already seen in Figures 1–3 between SDD and PD at large $\Delta\mathbf{r}^2$ values, can also be measured quantitatively by calculating the cross-correlation function R. This function is the sum over all R_i, where

$$R_i = \frac{(\mathrm{SDD}_i - \langle \mathrm{SDD} \rangle)}{\left\{\sum_j (\mathrm{SDD}_j - \langle \mathrm{SDD} \rangle)^2\right\}^{1/2}} \cdot \frac{(\mathrm{PD}_i - \langle \mathrm{PD} \rangle)}{\left\{\sum_j (\mathrm{PD}_j - \langle \mathrm{PD} \rangle)^2\right\}^{1/2}};$$

the subindices i and j are each one of all the bins (after the mean value of the distributions) used to plot the SDD and PD, $\langle \mathrm{SDD} \rangle$ and $\langle \mathrm{PD} \rangle$ are the averages over the i points of SDD_i and PD_i, respectively. Positive values of this function (possible values are $-1 \leq R \leq 1$) indicate that the two functions are positively correlated while negative values indicate anticorrelation; values close to zero mean that there is no correlation between them. In Figure 4, it can be seen that decreasing T improves the correlation between both distributions.

The confinement of the relaxation pathway suggested by Figures 2–4 represents an "entropic funnel" for the dynamical trajectories which can also be made explicit with the calculation of the Shannon entropy $H = N^{-1} \sum_{i=1}^{N} p(i) \cdot \log p(i)$, where $p(i)$ represents the probability that a given particle i has exceeded the mobility value θ in the different trajectories of the IC (calculated as the number of trajectories when such threshold displacement has been exceeded by the particle divided by the number of trajectories (200) of the IC). The function $p(i) \cdot \log p(i)$ presents a single maximum at probability $p = 1/e$ and is null at $p = 0.0$ and $p = 1.0$. Thus, a high value of Shannon entropy H (maximum value ≈ 0.16) would imply that most particles would present intermediate values in their probability of being mobile (of exhibiting very large displacements, larger than θ). In turn, a low value of H would mean that the particles would present high or low probabilities for such large mobility, without presence of significant intermediate behaviors. In other words, a low H value would mean that the sets of mobile particles (the ones comprised by the particles which exceed the value θ) would be similar for all the trajectories of the IC. Figure 5 shows that, consistently with the results of Figure 2, as T is lowered in the supercooled regime, the Shannon entropy decays as we approach T_c.

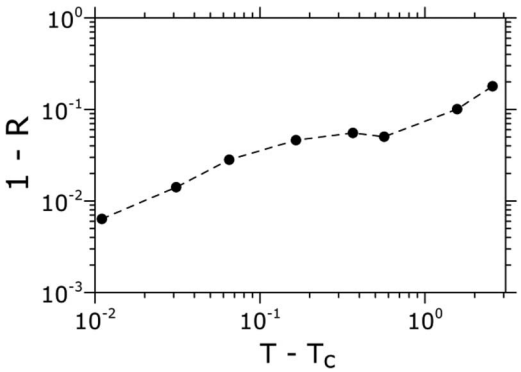

FIG. 4. Temperature dependence of the cross correlation function R between the squared-displacement distribution (SDD) and the propensity distribution (PD) for $t = 0.1 \cdot t^*$ after the mean value of the distributions.

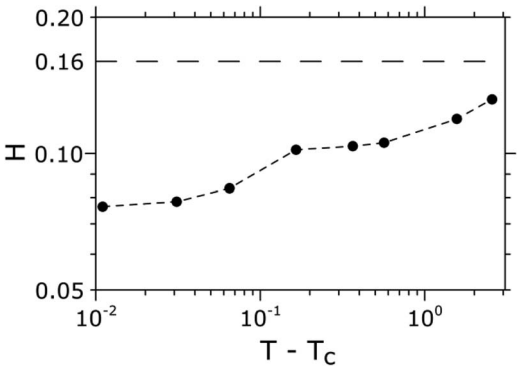

FIG. 5. Shannon entropy H as a function of temperature for $t = 0.1 \cdot t^*$. Dashed horizontal line: the maximum value of H is ≈ 0.16.

CONCLUSIONS

By means of extensive computations and calculations of detailed and specific dynamical quantities, our results shed a new additional light on the dynamical slowing down that occurs within the supercooled regime in a glass-forming system, while reconciling dynamical real-space, landscape-based, and structural-propensity descriptions. We have shown, by computing the excess of particle-mobility distributions over the corresponding propensity distributions, that while the dynamic trajectory has a rich menu of available relaxation alternatives at high temperatures (many different relaxing pathways made up by different mobile particles), glassy dynamics emerges at low temperatures since the relaxation pathway becomes increasingly confined to a common set of mobile particles. In other words, at high temperature there are many mobile particles (that can promote many different relaxation events) while the relaxation events can only choose from a reduced set of possible mobile particles as temperature decreases. This "entropic funnel" of relaxation pathways is furthermore made evident with the abrupt decay of the associated Shannon entropy.

ACKNOWLEDGMENTS

We have benefited from enlightening conversations with Professor Pablo Debenedetti. Financial support from MinCyT

and CONICET is gratefully acknowledged. J.A.R.F., M.A.F., and G.A.A. are research fellows of CONICET.

[1]C. A. Angell, J. Non-Cryst. Solids **131–133**, 13 (1991).
[2]S. Sastry, P. G. Debenedetti, and F. H. Stillinger, Nature (London) **393**, 554 (1998).
[3]M. D. Ediger, Annu. Rev. Phys. Chem. **51**, 99 (2000).
[4]T. R. Kirkpatrick, D. Thirumalai, and P. G. Wolynes, Phys. Rev. A **40**, 1045 (1989).
[5]E. R. Weeks, J. C. Crocker, A. C. Levitt, A. Schoeld, and D. A. Weitz, Science **287**, 627 (2000).
[6]J. D. Stevenson, J. Schmalian, and P. D. Wolynes, Nat. Phys. **2**, 268 (2006).
[7]D. Coslovich and G. Pastore, Europhys. Lett. **75**, 784 (2006).
[8]G. Biroli, J.-P. Bouchaud, K. Miyazaki, and D. Reichman, Phys. Rev. Lett. **97**, 195701 (2006).
[9]G. Biroli, J.-P. Bouchaud, A. Cavagna, T. Grigera, and P. Verrocchio, Nat. Phys. **4**, 771 (2008).
[10]A. Widmer-Cooper, H. Perry, P. Harrowell, and D. R. Reichman, Nat. Phys. **4**, 711 (2008).
[11]L. O. Hedges, R. L. Jack, J. P. Garrahan, and D. Chandler, Science **323**, 1309 (2009).
[12]K. Kim, K. Miyazaki, and S. Saito, Europhys. Lett. **88**, 36002 (2009).
[13]C. Brito and M. Wyart, J. Chem. Phys. **131**, 024504 (2009).
[14]R. Candelier, O. Dauchot, and G. Biroli, Phys. Rev. Lett. **102**, 088001 (2009).
[15]R. Candelier, A. Widmer-Cooper, J. K. Kummerfeld, O. Dauchot, G. Biroli, P. Harrowell, and D. R. Reichman, Phys. Rev. Lett. **105**, 135702 (2010).
[16]H. Tanaka, T. Kawasaki, H. Shintani, and K. Watanabe, Nat. Mater. **9**, 324331 (2010).
[17]W. Kob, S. Roldán-Vargas, and L. Berthier, Nat. Phys. **8**, 164 (2011).
[18]R. L. Jack and L. Berthier, Phys. Rev. E **85**, 021120 (2012).
[19]S. Karmakar, E. Lerner, and I. Procaccia, Physica A **391**, 1001 (2012).
[20]G. M. Hocky, T. E. Markland, and D. R. Reichman, Phys. Rev. Lett. **108**, 225506 (2012).
[21]W. Kob, S. Roldan-Vargas, and L. Berthier, Phys. Proc. **34**, 70 (2012).
[22]A. Malins, J. Eggers, C. P. Royall, S. R. Williams, and H. Tanaka, J. Chem. Phys. **138**, 12A535 (2013).
[23]P. Charbonneau and G. Tarjus, Phys. Rev. E **87**, 042305 (2013).
[24]W. Kob and L. Berthier, Phys. Rev. Lett. **110**, 245702 (2013).
[25]V. Lubchenko and P. G. Wolynes, Annu. Rev. Phys. Chem. **58**, 235 (2007).
[26]A. Heuer, J. Phys.: Condens. Matter **20**, 373101 (2008).
[27]A. Cavagna, Phys. Rep. **476**, 51 (2009).
[28]G. A. Appignanesi and J. A. Rodriguez Fris, J. Phys.: Condens. Matter **21**, 203103 (2009).
[29]D. Chandler and J. P. Garrahan, Annu. Rev. Phys. Chem. **61**, 191 (2010).
[30]L. Berthier and G. Biroli, Rev. Mod. Phys. **83**, 587 (2011).
[31]*Dynamical Heterogeneities in Glasses, Colloids and Granular Materials*, edited by L. Berthier, G. Biroli, J.-P. Bouchaud, L. Cipelletti, and W. van Saarloos (Oxford University Press, 2011).
[32]C. Donati, J. F. Douglas, W. Kob, S. J. Plimpton, P. H. Poole, and S. C. Glotzer, Phys. Rev. Lett. **80**, 2338 (1998).
[33]G. A. Appignanesi, J. A. Rodríguez Fris, R. A. Montani, and W. Kob, Phys. Rev. Lett. **96**, 057801 (2006).
[34]W. Kob and H. C. Andersen, Phys. Rev. E **51**, 4626 (1995).
[35]W. Kob and H. C. Andersen, Phys. Rev. Lett. **73**, 1376 (1994).
[36]U. Bengtzelius, W. Gotze, and A. Sjolander, J. Phys. C **17**, 5915 (1984).
[37]E. Leutheusser, Phys. Rev. A **29**, 2765 (1984).
[38]S. R. Nagel, in *Phase Transitions and Relaxation in Systems with Competing Energy Scales*, edited by T. Riste and D. Sherrington, (Kluwer Academic Publisher, Dordrecht, 1993), p. 259.
[39]B. Kim and G. F. Mazenko, Phys. Rev. A **45**, 2393 (1992).
[40]F. Mezei, J. Non-Cryst. Solids **131–133**, 317 (1991).
[41]W. Kob and H. C. Andersen, Phys. Rev. E **48**, 4364 (1993).
[42]W. Gotze, in *Liquids, Freezing and the Glass Transition*, Les Houches, Session LI, 1989, edited by J. P. Hansen, D. Levesque, and J. Zinn-Justin (North-Holland, Amsterdam, 1991), p. 287.
[43]W. Gotze and L. Sjogren, Rep. Prog. Phys. **55**, 241 (1992).
[44]R. A. L. Vallée, M. Van der Auweraer, W. Paul, and K. Binder, Phys. Rev. Lett. **97**, 217801 (2006).
[45]J. A. Rodríguez Fris, G. A. Appignanesi, and E. Weeks, Phys. Rev. Lett. **107**, 065704 (2011).
[46]B. Doliwa and A. Heuer, Phys. Rev. Lett. **91**, 235501 (2003).
[47]A. Widmer-Cooper, P. Harrowell, and H. Fynewever, Phys. Rev. Lett. **93**, 135701 (2004).
[48]Our results are in close accord with the results of Ref. 47 in which the distributions of particle propensity get progressively broader with supercooling. However, it has also been shown that approaching T_C the displacements distributions fatten additionally given the presence of another relaxation mechanism (probably a hopping process that might still be operative below T_C), a behavior not followed by the propensity distributions. This behavior occurs at the very long displacements which have low probability (they are evidenced in logarithmic plots): L. Berthier and R. L. Jack, Phys Rev. E **76**, 041509 (2007).
[49]J. A. Rodriguez Fris, L. M. Alarcón, and G. A. Appignanesi, J. Chem. Phys. **130**, 024108 (2009).
[50]G. A. Appignanesi, J. A. Rodriguez Fris, and M. A. Frechero, Phys. Rev. Lett. **96**, 237803 (2006).
[51]J. A. Rodriguez Fris, L. M. Alarcón, and G. A. Appignanesi, Phys. Rev. E **76**, 011502 (2007).
[52]P. Chaudhuri, L. Berthier, and W. Kob, Phys. Rev. Lett. **99**, 060604 (2007).